

## Optical Absorption of Arsenic-Doped Degenerate Germanium

J. I. PANKOVE

*RCA Laboratories, Princeton, New Jersey*

AND

P. AIGRAIN

*University of Paris, Paris, France*

(Received December 11, 1961)

The infrared transmission of degenerate arsenic-doped germanium was measured at liquid-helium and at room temperature. The 4.2°K data were used to calculate the energy gap of the degenerate material. For this, two operations were necessary: (1) to subtract the large effect of free carrier absorption, and (2) to calculate the absorption coefficient for the case of indirect transitions between two rigid parabolic bands one of which is partially occupied. A correction of the experimental data for the calculated Burstein shift shows that the indirect gap is considerably reduced  $[(93 \pm 4) \times 10^{-3}$  ev for  $4 \times 10^{19}$  As/cm<sup>3</sup>]. The data indicate that the direct gap at  $\mathbf{K} = (0,0,0)$  is also shrunk  $[(60 \pm 3) \times 10^{-3}$  ev for  $4 \times 10^{19}$  As/cm<sup>3</sup>]. Evidence is shown that momentum conservation in the indirect transition does not require phonons.

## I. INTRODUCTION

THERE has often been some concern about the rigidity of the band structure of semiconductors when a large concentration of impurities is introduced into the lattice. Early theoretical calculations<sup>1-3</sup> and impurity ionization measurements<sup>4,5</sup> have shown that at sufficiently large concentrations, impurities may form a band which merges with one of the intrinsic bands of the semiconductor. For a random or disordered distribution of impurities, the density of states at the band edges forms tails into the energy gap.<sup>6</sup> The band structure of a perfect crystal may be perturbed by the core potential of the specific impurity as well as by the localized strains (deformation potential)<sup>7</sup> induced by the slight misfit of the impurity. As the density of impurities increases, the perturbations overlap and tend to pull the bands to lower energies. From qualitative considerations, donors tend to depress the conduction band by virtue of their attractive potential. Holes, being heavier than electrons, are not as strongly affected by the repulsive potential of the donors; hence the valence band is only slightly perturbed. Ionized acceptors, on

the other hand, though they exert a repelling force on free electrons are not effective in changing the band structure because the electrons migrate to the undisturbed region around the acceptor. Hence, donors would tend to affect the band structure more strongly than acceptors. If the valence band is not shifted as strongly as the conduction band, the net effect is a shrinkage of the energy gap.

A typical example of gap shrinkage due to impurities is the case of indium-antimonide where the calculated Burstein effect<sup>8</sup> (the shift in optical threshold due to the rise of the Fermi level above the band edge) exceeds the observed threshold.<sup>9</sup> This discrepancy has been resolved by Aigrain and Des Cloizeaux<sup>2</sup> and by Stern and Talley<sup>3</sup> by allowing an impurity-dependent reduction of the energy gap.

In the case of germanium, the effect of impurities on the band structure has been reported previously,<sup>10</sup> it was concluded that an appreciable shrinkage of the energy gap occurs. Recently, reflectivity measurements on pure and doped germanium by Cardona and Sommers<sup>11</sup> have led to the same conclusion.

Preliminary absorption measurements on degenerate germanium which have already been reported<sup>12</sup> showed clearly a shift of the direct gap. These same data included a jog in the absorption curve at 0.48 ev which was then tentatively attributed to the onset of edge absorption. Since the publication of reference 12 it has been discovered that the jog was due to an instrumental malfunction.

In the present paper we shall present more recent data which not only confirm the previous interpretation of a reduced gap in degenerate germanium but which also suggest a new mechanism for optical transitions.

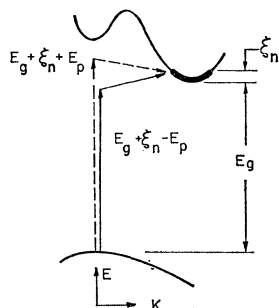


FIG. 1. Energy-momentum diagram for degenerate *n*-type germanium in the [111] direction. Two phonon-assisted transitions are shown to illustrate the usual photon absorption mechanism.

<sup>1</sup> W. Baltensperger, *Phil. Mag.* **44**, 1355 (1953).

<sup>2</sup> P. Aigrain and J. des Cloizeaux, *Compt. rend.* **241**, 859 (1955).

<sup>3</sup> F. Stern and R. M. Talley, *Phys. Rev.* **100**, 1638 (1955).

<sup>4</sup> J. Bardeen and G. L. Pearson, *Phys. Rev.* **75**, 865 (1949).

<sup>5</sup> P. P. Debye and E. M. Conwell, *Phys. Rev.* **93**, 693 (1954).

<sup>6</sup> R. H. Parmenter, *Phys. Rev.* **97**, 587 (1955).

<sup>7</sup> C. Benoit-à-la-Guillaume, *Ann. phys.* **5**, 1187 (1959).

<sup>8</sup> E. Burstein, *Phys. Rev.* **93**, 632 (1954).

<sup>9</sup> M. Tanenbaum and H. B. Briggs, *Phys. Rev.* **91**, 1501 (1953).  
H. J. Hrostowski, G. H. Wheatley and W. F. Flood, *Phys. Rev.* **95**, 1683 (1954).

<sup>10</sup> J. I. Pankove, *Ann. phys.* **6**, 331 (1961).

<sup>11</sup> M. Cardona and H. S. Sommers, *Phys. Rev.* **122**, 1382 (1961).

<sup>12</sup> J. I. Pankove, *Phys. Rev. Letters* **4**, 454 (1960).

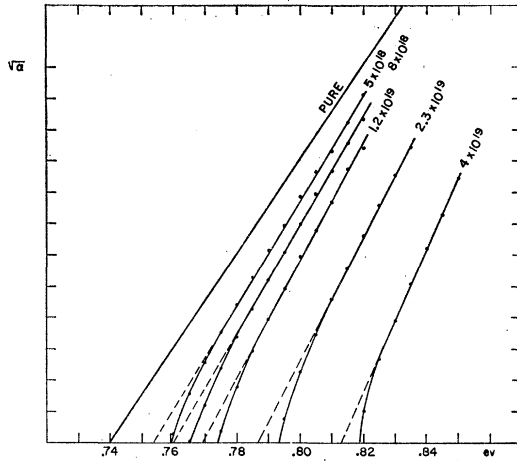


FIG. 2. Calculated effect of the filling of the conduction band on optical absorption in germanium at 4.2°K.

We shall first calculate the optical absorption characteristic of a degenerate material based on the rigid-band model. Then, we shall describe the experimental method and the results obtained, and show how the actual situation differs from the prediction. Finally we shall discuss an interpretation of these results and tie it with other types of experimental observations.

## II. OPTICAL TRANSITIONS BETWEEN PARABOLIC BANDS IN A DEGENERATE SEMICONDUCTOR

Figure 1 shows schematically the band structure of germanium in energy-momentum space in the [111] direction. To indicate that this is degenerate *n*-type germanium the bottom of the conduction band is shown by a heavy line over the occupied states, those below the Fermi level. Transitions between the top of the valence band and the [111] valley of the conduction band are indirect transitions. In these transitions, momentum conservation can be satisfied by two processes: (1) phonon cooperation, (2) impurity scattering.<sup>13</sup>

In pure material, phonon absorption and emission are the only means for conserving momentum. At low temperatures, only phonon emission occurs. In this case, the photon absorbed differs from the energy separating the initial and final states by the energy of the phonon involved (mostly 0.008 eV—the transverse acoustic phonon).

On the other hand, if impurity scattering conserves momentum, which may occur in degenerate materials, no phonon is involved and the photon energy truly represents the separation between initial and final states. In this case, however, one might expect that the matrix element linking the two states be proportional to the impurity concentration. This would cause the absorption coefficient for transitions between a set of states to increase with the impurity concentration. The data below will corroborate this interpretation.

<sup>13</sup> Since this writing, Haas has pointed out a third process: electron-electron scattering; Phys. Rev. **125**, 1965 (1962).

Regardless of the process by which momentum is conserved, the absorption coefficient  $\alpha(h\nu)$  for indirect transitions is proportional to the product of initial and final densities of states integrated over all the pairs of states separated by a given  $h\nu$ . A reasonable agreement between theory and experiment has been obtained by Macfarlane and Roberts<sup>14</sup> in the case of nondegenerate germanium when they assumed that the matrix element for these transitions is independent of energy. With the same assumption and for the case of parabolic bands one gets the following expression for the absorption coefficient of degenerate germanium:

$$\alpha = F(N) \left\{ A_a \int_0^{E_{vm}} \frac{(E_{vm} - E_v)^{\frac{1}{2}} E_v^{\frac{1}{2}}}{1 + \exp[(\xi - E_{vm} + E_v)/kT]} dE_v + A_e \int_0^{E_{vm}^*} \frac{(E_{vm}^* - E_v)^{\frac{1}{2}} E_v^{\frac{1}{2}}}{1 + \exp[(\xi - E_{vm}^* + E_v)/kT]} dE_v \right\}, \quad (1)$$

where  $F(N)$  is a constant dependent on the impurity concentration  $N$ ;  $E_{vm} = h\nu - (E_g - E_p)$ , phonon absorption;  $E_{vm}^* = h\nu - (E_g + E_p)$ , phonon emission;  $E_g$  = energy gap;  $E_p$  = energy of the phonon involved;  $A_a, A_e$  = relative probability for, respectively, absorbing and emitting a phonon (this is strongly temperature dependent);  $\xi$  = position of the Fermi level with respect to the band edge; and  $E_v$  = variable of integration.

For transitions to states substantially above the Fermi level, the exponents in Eq. (1) are large and negative and therefore the exponential drops out. Then, the solution of Eq. (1) is of the form

$$\alpha = F(N) \{ A_a [h\nu - (E_g - E_p)]^2 + A_e [h\nu - (E_g + E_p)]^2 \}. \quad (2)$$

At low temperature, the phonon-emission term is dominant, hence

$$\alpha^{\frac{1}{2}} = F(N)^{\frac{1}{2}} A_e^{\frac{1}{2}} [h\nu - (E_g + E_p)]. \quad (3)$$

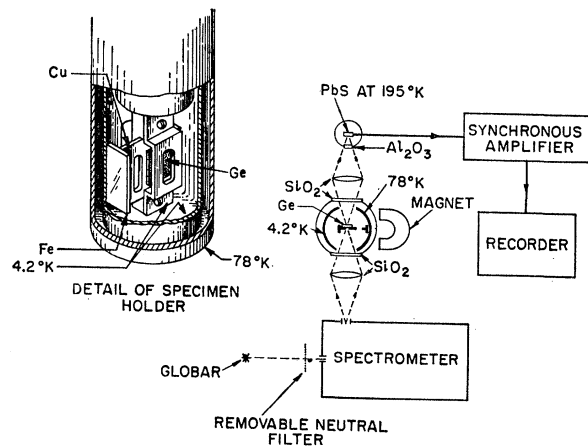


FIG. 3. Experimental setup.

<sup>14</sup> G. G. Macfarlane and V. Roberts, Phys. Rev. **97**, 1714 (1955.)

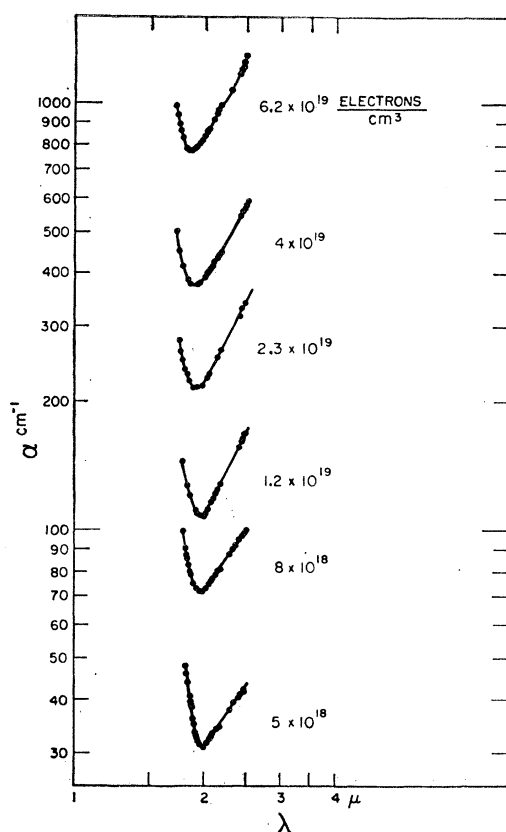


FIG. 4. Absorption coefficient of arsenic-doped germanium at 300°K.

This is the basis for the Macfarlane-Roberts<sup>14</sup> method of plotting absorption data:  $\alpha^{1/2}$  plotted against  $h\nu$  gives a straight line intercepting the  $h\nu$  axis at  $E_g + E_p$  in the case of pure germanium and at some higher value in the case of degenerate germanium as will soon be shown by the solution of Eq. (1).

A calculation of expression (1) at 4.2°K was run on an IBM 650 Computer neglecting the phonon-absorption term, assuming  $F(N)$  constant and taking arbitrarily  $E_g + E_p = 0.740$  ev. The result of the calculation, plotted à la Macfarlane and Roberts, i.e., as  $\alpha^{1/2}$  vs  $h\nu$ ,

TABLE I. Impurity concentration, thickness and reflectivity of the specimens.

Concentration <sup>a</sup> As/cm <sup>2</sup>	Thickness (microns)	Reflectivity coefficient
$8 \times 10^{13}$ ("Pure")	56 and 1210	0.360
$5 \times 10^{18}$	170	0.350
$8 \times 10^{18}$	56	0.372
$1.2 \times 10^{19}$	56	0.366
$2.3 \times 10^{19}$	53	0.355
$4 \times 10^{19}$	58.5	0.350
$6.2 \times 10^{19}$	48	0.360 <sup>b</sup>

<sup>a</sup> The concentration was determined by a Hall effect measurement, on nearby slices from the same crystal. It is assumed that the electron concentration is equal to the arsenic concentration, a relationship found true for other crystals grown in the same manner in a range of up to  $4 \times 10^{19}$ .

<sup>b</sup> Assumed.

is reproduced on Fig. 2. For pure germanium, a straight line is obtained which intercepts the axis at the value  $E_g + E_p$ . The straight line characterizes the fact that the transitions are indirect and occur between parabolic bands in which case  $\alpha$  is proportional to  $(h\nu)^2$ . As the impurity concentration increases, the threshold shifts to higher energies ( $E_g + E_p + \xi$ ) since the states below the Fermi level are forbidden. Furthermore, although at higher energies (beyond the range shown in Fig. 2) all the curves tend to be straight lines parallel to the pure germanium case, the absorption coefficient decreases as the degree of degeneracy increases. This decrease in the absorption coefficient results from the reduction in the number of transitions that can take place since more final states are forbidden by the filling of the band. This is then the picture based on a rigid band structure with impurities contributing only an abundance of free carriers.

### III. EXPERIMENTAL METHOD

Arsenic-doped germanium wafers, lapped and polished consisted of those listed in Table I. The specimen was mounted over one of two identical apertures in a copper plate placed in a special holder at the bottom of a "Hofman" liquid-helium Dewar. The copper plate could be moved by remote magnetic control so that either the specimen or the aperture would be positioned in the infrared beam. The Dewar was placed in the exit path of a double-pass Perkin-Elmer spectrometer (model 112) equipped with a quartz prism. A Globar powered by a regulated power supply was the source of radiation. The detector consisted of a lead-sulfide photoconductor cooled with dry ice in acetone. The installation is illustrated in Fig. 3.

The data were gathered point-by-point with the

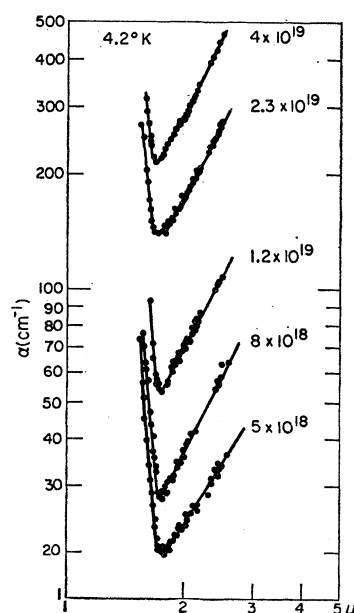


FIG. 5. Absorption coefficient of arsenic-doped germanium at 4.2°K.

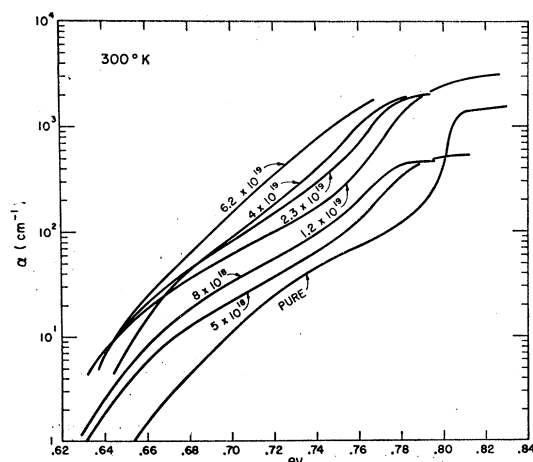


FIG. 6. Band-to-band absorption coefficient of arsenic-doped germanium at 300°K obtained from Fig. 4 by subtracting the free carrier absorption from the measured value. These data not being corrected for reflectivity are shown only for the purpose of illustrating qualitatively the shift of the direct transition and the increase of the absorption coefficient with increasing arsenic concentration.

spectrometer set at a given wavelength, sometimes for as long as 10 min to obtain the desired accuracy (0.5%). The output of the detector was fed to a synchronous amplifier the output of which was recorded on an instrument equipped with a ball-and-disk integrator so that an average value of the signal could be obtained by an integration method when desired.

The sample-in-sample-out method of determining the transmission eliminated any possible concern over long term stability of the ir source. Calibrated neutral filters could be inserted in the beam during the sample-out period to greatly increase the measurable range of transmission without saturating the detector. All the measurements corresponding to an absorption coefficient of less than 500 cm<sup>-1</sup>, i.e., most of the measurements, were made with a slit width of 80 μ (resolution better than 0.0015 eV).

The absorption coefficient  $\alpha$  was calculated from the expression which takes into account multiple reflections:

$$T = \frac{(1-R)^2 e^{-\alpha x}}{1 - R^2 e^{-2\alpha x}}, \quad (4)$$

where  $T$  is the measured transmission,  $x$  the sample thickness and  $R$  the reflectivity.

Transmission measurements were made both at room temperature and at 4.2°K but only the 4.2°K data were subjected to the correction for actual reflectance, whereas for the 300°K data (which had been measured first) a reflectivity of 0.360 had been assumed.

The stability of the spectrometer's setting was periodically verified by a calibration test with the green line of a mercury arc.

The reflectivity in the range  $2 < \lambda < 2.5 \mu$ , was measured at room temperature by comparison with an aluminized mirror; these data were corrected for multiple internal reflections in the various samples. They are listed in Table I. The reflectivity was assumed constant over the range of interest ( $\lambda < 2.5 \mu$ )—although this assumption is not correct ( $R$  increases with decreasing wavelength in the edge absorption range) it will be shown in Sec. IV that our results do not depend significantly on this assumption.

#### IV. RESULTS

Part of the data obtained at 300°K and at 4.2°K is shown in Figs. 4 and 5. The part omitted for the sake of clarity in these figures, but measured and used later on, is the continuation of the curves to shorter wavelengths. It is evident that two absorption processes take place: (1) free-carrier absorption at long wavelength varying roughly as  $\lambda^2$  over the range investigated; (2) edge absorption at short wavelength, increasing with decreasing  $\lambda$ .

Free carrier absorption increases with the carrier concentration and approximately with the square of the wavelength. In order to abstract the edge absorption from the measured data, free carrier absorption was extrapolated to the region of edge absorption with the assumption that the  $\lambda^n$  dependence ( $n \approx 2$ ) is still obeyed over that range. Then, the extrapolated free carrier absorption was subtracted from the measured absorption coefficient to yield the coefficient characteristic of edge absorption. The result is shown in Figs. 6 and 7.

It must be pointed out at this time that the assumption of a constant reflectivity (independent of  $\lambda$ ), which was made in Sec. III, is not critical in determining the absorption coefficient for the band-to-band transitions. As a check on the acceptability of this assumption, the

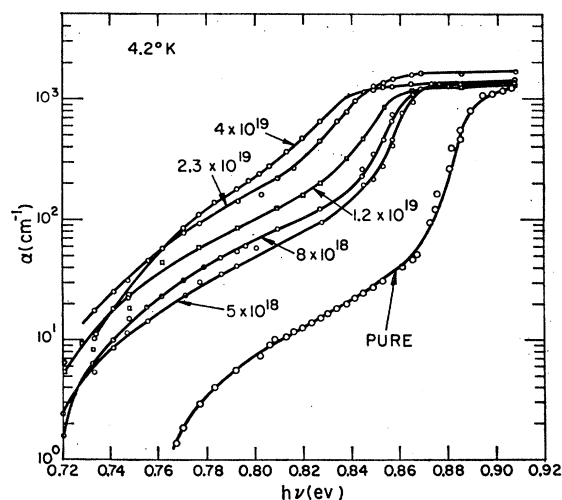


FIG. 7. Band-to-band absorption coefficient of arsenic-doped germanium at 4.2°K obtained from the data of Fig. 5.

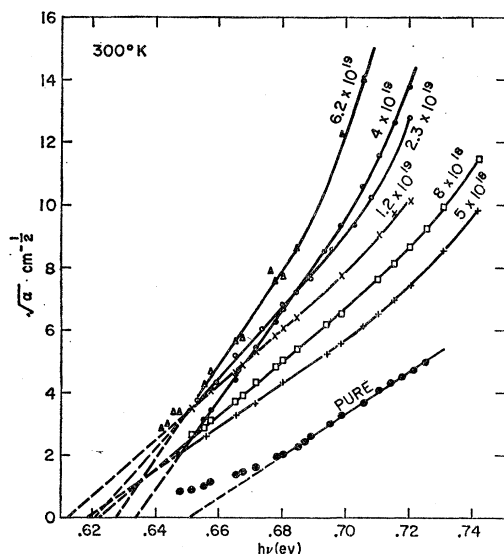


FIG. 8. Macfarlane-Roberts type plot applied to the data of Fig. 6.

data of Cardona, Paul and Brooks<sup>15</sup> (giving the dependence of the index of refraction on wavelength and temperature) were used to compute the reflectivity of the specimen doped with  $4 \times 10^{19}$  As/cm<sup>3</sup>. Although the measurements of Cardona *et al.* were made on pure germanium, it is believed that a similar variation would be found in the degenerate material. However, for our purpose this assumption seems un consequential because, although the total absorption is affected by the value of the reflection coefficient in the region of highest transmittance, the absorption coefficient for band-to-band transitions remains unchanged.

The curves of Figs. 6 and 7 show two types of transitions: those between the top of the valence band and the indirect valley of the conduction band at  $\mathbf{K}=(1,1,1)$  (the indirect gap) and those between the top of the valence band and the direct valley of the conduction band at  $\mathbf{K}=(0,0,0)$  (the direct gap). The latter is identified by the fast rising region which precedes the knee of the curve at high energy. The existence of the two processes is most pronounced in the curves for the pure specimen. The only significant conclusion which may be derived from Figs. 6 and 7 is that the direct gap decreases considerably with increasing doping. It is premature to judge the rest of the curve because, as mentioned in Sec. II, impurity scattering would cause, in this representation, an apparent shift of the curves to a lower energy since the absorption coefficient for a given transition would be proportional to the impurity concentration. Further analysis of the indirect gap region will follow presently.

In Sec. II we have shown that the square root of the absorption coefficient may be expected to be propor-

tional to the photon energy. At 300°K two branches are expected: that due to the absorption and that due to the emission of phonons (at least in the case of pure material). The data for edge absorption plotted in Figs. 8 and 9 show that the straight lines predicted by expression (3) are indeed obtained. The deviation from the straight line at low values of  $\alpha^{1/2}$  (below  $\alpha^{1/2}=3$ ) is due to the inaccuracy in determining low values of  $\alpha$  which are obtained by taking the small difference between two large numbers. The deviation from the straight line at large values of  $\alpha^{1/2}$  is due to the onset of direct transitions [at  $\mathbf{K}=(0,0,0)$ ]. It can be seen that for degenerate materials the intercept with the  $h\nu$  axis occurs at a lower energy than for the pure specimen.

The two branches corresponding to phonon emission and absorption are clearly seen in Fig. 8 for pure germanium. In the case of degenerate material, low accuracy for small values of  $\alpha$  prevent any conclusion about phonon processes. For simplicity's sake, only the low temperature data will be interpreted since, in this case, phonon absorption does not play a significant part.

The slope of these lines should yield some information about  $F(N)$ . In Sec. II we suggest that, for lack of better knowledge,  $F(N)$  should be proportional to  $N$ . In this instance, a differentiation of (3) gives

$$d\alpha^{1/2}/dh\nu \propto N^{1/2}. \quad (5)$$

Figure 10 shows that the slope  $d\alpha^{1/2}/dh\nu$  plotted against  $N$  on a log-log scale is in fact  $\frac{1}{2}$ . This tends to confirm the model of impurity scattering<sup>16</sup> as the momentum con-

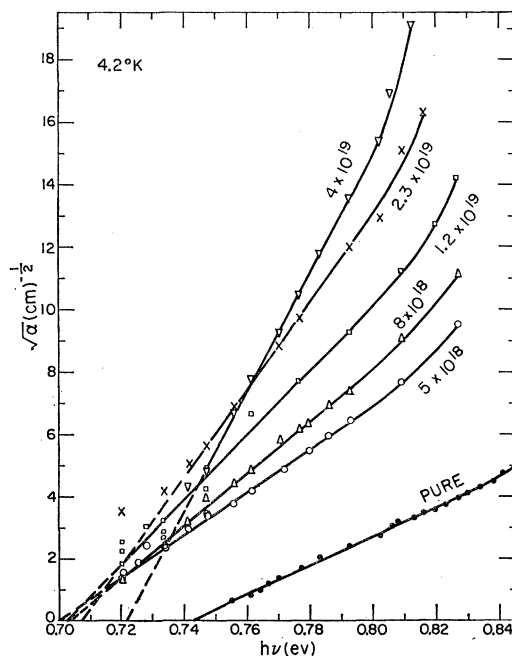


FIG. 9. Macfarlane-Roberts type plot applied to the data of Fig. 7.

<sup>15</sup> M. Cardona, W. Paul and H. Brooks, J. Phys. Chem. Solids 8, 204 (1959).

<sup>16</sup> Or that of electron-electron scattering as per Haas.

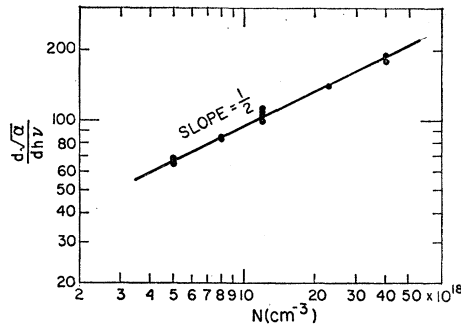


FIG. 10. Variation of the slopes of the curves in Fig. 9 as a function of carrier concentration.

serving process in the indirect transition. The absence of phonons in tunneling from arsenic-doped degenerate germanium has already been observed by Holonyak *et al.*,<sup>17</sup> and direct transitions at  $K=0$  from arsenic levels to the valence band have been observed in emission measurements by Benoit-la-Guille and Parodi.<sup>18</sup> If phonons are not needed, the optical threshold should be located at the actual band edge plus the calculated shift due to the filling of the band. This enables us to evaluate the indirect gap  $E_g$  of the degenerate material:

$$E_g = h\nu_0 - \epsilon, \quad (6)$$

where  $h\nu_0$  is the intercept at the abscissa for the extrapolated curve  $\alpha^{1/2}$  of Fig. 9 and  $\epsilon$  is the shift due to the filling of the band determined from Fig. 2 by taking the difference between the abscissal intercepts of the straight line approximation for the impure specimen and the abscissal intercept for the pure case. In Table II we have listed the values for  $\xi$ ,  $h\nu_0$ ,  $\epsilon$ ,  $E_g$ , and  $\Delta_1$  which is the shrinkage of the gap due to doping defined as:  $\Delta_1 = E_{g0} - E_g$ , where  $E_{g0}$  is the gap of pure germanium (0.740 eV).<sup>19</sup>

The limits of incertitude entered in Table II reflect the maximum possible error due to the scatter of the free carrier absorption data. Since, in most cases, slightly different extrapolations for free carrier absorp-

TABLE II. Properties of arsenic-doped degenerate germanium at 4.2°K as determined in the present work.

$N$ As/cm <sup>3</sup>	$\xi$ (10 <sup>-3</sup> eV)	$h\nu_0$ (10 <sup>-3</sup> eV)	$\epsilon$ (10 <sup>-3</sup> eV)	$E_g$ (10 <sup>-3</sup> eV)	$\Delta_1$ (10 <sup>-3</sup> eV)
$5 \times 10^{18}$	19.5	$695 \pm 5$	14	$681 \pm 5$	59
$8 \times 10^{18}$	26.5	$703 \pm 1$	20	$683 \pm 1$	57
$1.2 \times 10^{19}$	34.5	$703 \pm 6$	29	$674 \pm 6$	66
$2.3 \times 10^{19}$	53.5	$707.5 \pm 1$	47	$660.5 \pm 1$	79.5
$4 \times 10^{19}$	78	$720 \pm 4$	73	$647 \pm 4$	93

<sup>17</sup> N. Holonyak, I. A. Lesk, R. N. Hall, J. J. Tiemann, and H. Ehrenreich, Phys. Rev. Letters 3, 167 (1959).

<sup>18</sup> C. Benoit-la-Guille and O. Parodi, *Proceedings of the International Conference on Semiconductor Physics* (Czechoslovakian Academy of Sciences, Prague, 1961), p. 426.

<sup>19</sup> J. R. Haynes, M. Lax and W. F. Flood, J. Phys. Chem. Solids 8, 392 (1959).

TABLE III. Position of the Fermi level at 4.2°K and shrinkage of the energy gap at  $K=(0,0,0)$  and  $K=(1,1,1)$ .

$N$ As/cm <sup>3</sup>	$\xi$ (10 <sup>-3</sup> eV)	$\Delta_0$ (10 <sup>-3</sup> eV)	$\Delta_1$ (10 <sup>-3</sup> eV)
$5 \times 10^{18}$	19.5	$28 \pm 3$	$59_{-10}^{+5}$
$8 \times 10^{18}$	26.5	$32 \pm 3$	$57_{-6}^{+1}$
$1.2 \times 10^{19}$	34.5	$38 \pm 3$	$66_{-11}^{+6}$
$2.3 \times 10^{19}$	53.5	$52 \pm 3$	$79.5_{-6}^{+1}$
$4.0 \times 10^{19}$	78	$60 \pm 3$	$93_{-9}^{+4}$

tion are possible into the region of edge absorption, different band-to-band absorption coefficient are obtainable. However the edge absorption grows very rapidly at shorter wavelengths and therefore the incertitude in the extrapolated value of the free carrier absorption has a relatively small effect on the determination of  $h\nu_0$ . Since the experimental intercept  $h\nu_0$  for pure germanium is 0.005 eV lower than predicted by theory ( $E_g + E_p = 0.748$  eV) a systematic error of -0.005 eV may be suspected; then the above values of  $\Delta_1$  would be lowered correspondingly.

From the steep rising portion of the curves, on Fig. 7 it is possible to estimate the change in the energy gap at  $K=(0,0,0)$ . The abscissa at which the edge absorption coefficient equals 900 cm<sup>-1</sup> is subtracted from the corresponding value for pure germanium. This difference is tabulated as  $\Delta_0$  in Table III together with the  $\Delta_1$  of Table II. The range of accuracy in  $\Delta_0$  is determined by the spectral resolution.

The data of Table III suggest that both conduction band valleys at  $K=(0,0,0)$  and at  $K=(1,1,1)$  move closer to the valence band, the valley at  $K=(1,1,1)$  being more strongly affected than the valley at  $K=(0,0,0)$ . The shrinkage of the gap at these two regions is plotted in Fig. 11.

## V. CONCLUSIONS

The operations performed above on the absorption data suggest that in degenerate germanium doped with arsenic, the energy gap is shrunk by somewhat more

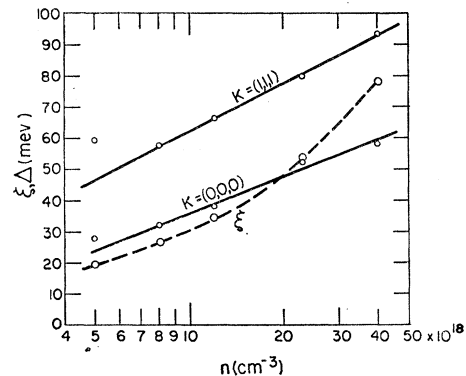


FIG. 11. Shrinkage ( $\Delta$ ) of the energy gap at  $K=(1,1,1)$  and at  $K=(0,0,0)$  and penetration ( $\xi$ ) of the Fermi level into the conduction band at 4.2°K as a function of doping.

than the rise of the Fermi level above the conduction band. This may be as much as a 15% change in the band gap (for the most heavily doped specimen studied). This agrees qualitatively with many of the observations previously reported on degenerate germanium<sup>10,20</sup>: reduced barrier height for hole injection into degenerate *n*-type germanium, reduced energy in reflectivity data for *L*-type transitions<sup>11</sup> (here there is also quantitative agreement), reduced barrier height in capacitance measurement,<sup>21</sup> shift of the emission spectrum to lower energy. However the present work does not explain all of the observations made during emission experiments. For example the presence of two emission mechanisms at different energies, both lower than the gap of pure germanium, does not show a counterpart in the absorption measurement. Although this appears as a lack of

concordance between the two sets of experiments, it is not necessarily an inconsistency since the two methods may not be equally sensitive in revealing the same details of the band structure.

Sommers<sup>22</sup> has made another interpretation of various measurements on degenerate germanium with the conclusion that the energy gap is only  $30 \times 10^{-3}$  eV less than in the unperturbed lattice. Since the present measurements lead to quite a different conclusion, the problem of interpreting the various measurements on degenerate germanium is again an open question.

Another conclusion is that the dominant electron scattering mechanism is not a phonon scattering process but rather one dependent on the electron concentration.

#### ACKNOWLEDGMENT

It is with gratitude that we acknowledge the diligent assistance of J. E. Berkeyheiser.

<sup>22</sup> H. S. Sommers, *Phys. Rev.* **124**, 1101 (1961).

<sup>20</sup> D. Meyerhofer, G. A. Brown, and H. S. Sommers (to be published).

<sup>21</sup> A. G. Chynoweth, W. L. Feldman, C. A. Lee, R. A. Logan, G. L. Pearson, and P. Aigrain, *Phys. Rev.* **118**, 425 (1960).

## Field Dependence of the Electric Susceptibility of Ionic Crystals

F. NINIO

*School of Physics, University of New South Wales, Kensington, Australia*

(Received December 4, 1961)

An attempt has been made to estimate the field dependence of the electric susceptibility of simple ionic crystals by considering a linear chain of alternating positive and negative ions interacting only through nearest neighbors. The pressure and temperature dependence have also been included to compare with experiment and thereby to give some indication of the reliability of the model. It is found that the dependence on all three parameters is directly related to the anharmonicity in the vibrational motion.

### 1. INTRODUCTION

FOR the explanation of many properties of crystals it is often sufficient to expand the potential energy as a Taylor series in the displacements of the lattice particles about their equilibrium positions, and to retain only the terms involving the second derivatives. With this "harmonic" approximation one may show in particular that under electric fields, the polarization of a simple ionic crystal is proportional to the field. This relation in turn may be regarded as a first-order Taylor expansion in the field, so that for intense fields one would expect a dependence of the polarization on the cube of the field. This additional dependence would correspond to the inclusion of higher derivatives (the "anharmonic" terms) in the expansion of the potential energy.

In this paper, we attempt to estimate this field dependence for ionic crystals by deriving an expression for the electric susceptibility of a linear chain of alter-

nating positive and negative point ions interacting only with nearest neighbors, and then assuming, after suitable adjustment of dimensions, that this expression actually holds for the 3-dimensional crystal. The problem of field dependence has been treated in general by O'Dwyer<sup>1</sup> but the calculation below gives an expression in terms of constants related directly to the anharmonicity.

Unfortunately there are no data with which to compare the result. However, in the derivation, the temperature and pressure dependence are included also. An order of magnitude calculation for these, in the case of NaCl, then gives figures which agree roughly with values by Bretscher<sup>2</sup> and Mayburg.<sup>3</sup> This gives some indication of the reliability of the model for estimating the order of magnitude for field dependence.

<sup>1</sup> J. J. O'Dwyer, *Proc. Phys. Soc. (London)* **A64**, 1125 (1951).

<sup>2</sup> E. Bretscher, *Trans. Faraday Soc.* **30**, 684 (1934).

<sup>3</sup> S. Mayburg, *Phys. Rev.* **79**, 375 (1950).